

1 **Male-Specific Protein Disulphide Isomerase Function is Essential for *Plasmodium***
2 **Fertilization and Transmission**

3

4

5 Fiona Angrisano¹, Katarzyna A. Sala¹, Sofia Tapanelli¹, George K. Christophides¹, Andrew M.
6 Blagborough^{1, 2*}

7

8

9

10 ¹ Department of Life Sciences, Imperial College of Science, Technology and Medicine,
11 London, SW7 2AZ, United Kingdom.

12 ²Lead Contact

13 * Correspondence: a.blagborough@imperial.ac.uk

14

15

16

17

18

19

20

21

22

23

24

25

26 **Keywords:** Malaria, *Plasmodium*, transmission, gamete, fertilization.

27

28

29 **Summary:**

30 Inhibiting transmission of *Plasmodium* is an essential strategy in malaria eradication, and the
31 biological process of gamete fusion during fertilization is a proven target for this approach.
32 The lack of knowledge of the mechanisms underlying fertilization have been a hindrance in
33 the development of transmission-blocking interventions. Here we describe a protein disulphide
34 isomerase essential for malarial transmission (*PDI-Trans*/PBANKA_0820300) to the
35 mosquito. We show that *PDI-Trans* activity is male-specific, surface expressed, essential for
36 fertilization/transmission, and exhibits disulphide isomerase activity which is up-regulated
37 post-gamete activation. We demonstrate that *PDI-Trans* is a viable anti-malarial drug and
38 vaccine target blocking malarial transmission with the use of the PDI inhibitor bacitracin
39 (98.21%/92.48% reduction in intensity/prevalence), and anti-*PDI-Trans* peptide antibodies
40 (66.22%/33.16% reduction in intensity/prevalence). To our knowledge, these results provide
41 the first primary evidence that protein disulphide isomerase function is essential for malarial
42 transmission, and emphasize the potential of anti-PDI agents to act as anti-malarials,
43 facilitating the future development of novel transmission-blocking compounds or vaccines.

44

45

46

47

48

49

50

51

52

53

54

55

56

57 **Introduction:**

58

59 Malaria remains a major global health challenge with an estimated 216 million new cases and
60 445,000 deaths in 2016 [1]. Current tools have substantially reduced the global burden of
61 disease, but recent progress has stalled [1], and it is widely accepted that a range of new tools
62 will be needed to achieve malaria elimination [2]. The causative agent of malaria, the
63 protozoan parasite *Plasmodium*, is transmitted almost exclusively by mosquitoes of the genus
64 *Anopheles*. Transmission of *Plasmodium* from humans to mosquitoes is entirely dependent
65 on the presence of sexually committed gametocytes in circulating blood, which rapidly undergo
66 the process of activation and differentiate into male (micro) and female (macro) gametes upon
67 uptake by the mosquito within a blood meal. The essential process of fertilization is then
68 initiated by gamete adhesion, followed by membrane fusion [3,4]. A small number of proteins
69 have been previously been implicated in plasmodial fertilization; the 6-Cys protein family
70 members P48/45, P47 and P230 have been shown to have a demonstrable role in the mutual
71 recognition and adhesion of micro- and macro-gametes [5-7], whereas the conserved male-
72 specific Class II fusion protein HAP2/GCS1 has been shown to be the key driver of membrane
73 fusion by mediating merger of lipid bilayers [3-4]. Following successful fertilization, resulting
74 zygotes develop into motile ookinetes, establishing infection in the insect host by migration
75 and invasion of the mosquito midgut, allowing for the progression of the parasitic lifecycle.
76 Despite the obvious biological importance of parasitic transmission and its proven previous
77 targeting as a potential point to disrupt the parasitic lifecycle with multiple therapeutics [8], our
78 knowledge of the cellular and molecular mechanisms underlying fertilization and subsequent
79 zygote formation in *Plasmodium* are surprisingly sparse.

80

81 It is widely recognized that to achieve malarial eradication, it will be necessary to use
82 interventions that inhibit the transmission of parasites from humans to mosquitoes [2]. A
83 potential manner of achieving this is by targeting *Plasmodium* using transmission-blocking
84 interventions (TBIs); i.e. transmission blocking vaccines (TBVs), or transmission blocking

85 drugs (TBDs) against parasitic sexual stages [9]. Antibodies targeted to three of the five
86 currently proven, potent TBV targets have confirmed localization to proteins found on the
87 surface of the plasma membrane of the gametes [10-20], clearly indicating the potential value
88 of targeting this stage of the parasite lifecycle. Additionally, multiple anti-malarial compounds
89 have been demonstrated to have activity against this parasitic stage [21-25]. In summary, the
90 comparatively short life span, increased fragility and availability of proven surface-localized
91 proteins on the male gamete of *Plasmodium* make targeting this gamete stage of the lifecycle
92 a potential method of inhibiting transmission [26,27]. Similarly, potent TBIs targeting the
93 parasitic ookinete post-fertilization are well characterized in multiple vaccine and drug studies
94 [16,17,25, 28-30].

95

96 Protein Disulphide Isomerase (PDI) (EC: 5.3.4.1) is a multifunctional member of the
97 thioredoxin superfamily of redox proteins, characterized by the presence of the $\beta\alpha\beta\alpha\beta\alpha\beta\alpha$
98 fold [31]. PDIs typically have three catalytic activities; disulphide isomerase, thiol-disulphide
99 oxidoreductase, and redox-dependent chaperone. PDI homologues have been identified in
100 multiple species, where they are “classically” located in the endoplasmic reticulum (ER) and
101 facilitate the folding and assembly of secretory and membrane proteins within the lumen [32].
102 In *Plasmodium*, a small number of proteins have been putatively identified (by sequence
103 homology) as PDI-like molecules in *Plasmodium falciparum*, *vivax*, *knowlesi*, *berghei* and
104 *yoelii* [33,34]. Conclusive demonstration of PDI activity has currently only been demonstrated
105 with PF3D7_0827900/PDI-8 [33], with transcription and translation demonstrated in asexual
106 blood schizonts, gametocytes and sporozoites. Knowledge regarding the process of
107 disulphide bond-dependent protein folding in *Plasmodium* is scarce. Similarly, to target the
108 sexual stages of the malaria parasite further, a deeper understanding of transmission and
109 specifically, the mechanism of fertilization within *Plasmodium* is vital, and offers the potential
110 for the development of new, effective anti-malarial TBIs. Here, we describe the identification,
111 characterization and role of a protein disulphide isomerase essential for malarial transmission
112 (*PDI-Trans*/PBANKA_0820300) to the mosquito host in *P. berghei*. We demonstrate that *PDI-*

113 *Trans* is transcribed and translated across the entire parasitic lifecycle, but exhibits activity at
114 the sexual stages of the lifecycle, when fertilization of gametes occurs. We show that *PDI-*
115 *Trans* is male specific, essential for successful fertilization/transmission, and exhibits
116 disulphide isomerase function which is up-regulated post-gamete activation. Furthermore, we
117 show that *PDI-Trans* is a viable anti-malarial drug and vaccine target, expressed on the
118 surface of the sexual stages of *Plasmodium*, by blocking malarial transmission with the use of
119 repurposed compounds that target PDI activity, and anti- *PDI-Trans* peptide antibodies. These
120 results demonstrate that protein disulphide isomerase function is essential for malarial
121 transmission, emphasize the potential of anti-PDI agents to act as anti-malarials, and
122 demonstrate the potential utility of rationally selected targets to facilitate the development of
123 novel anti-malarial transmission-blocking interventions.

124

125 **Results:**

126 ***PDI-Trans is located on the surface on the transmission stages of P. berghei***

127

128 Previous proteomic analysis of a *P. berghei* male gamete proteome generated in [35] followed
129 by advanced bioinformatics analysis encompassing a suite of functional and localization-
130 based algorithms [36] identified the expression of *PDI-Trans* (PBANKA_0820300) in the male
131 gamete, and suggested that the resulting transmembrane protein was potentially located on
132 the surface of the plasma membrane of male gametes. A brief analysis of *PDI-Trans* is
133 described within [37], where following a BarSeq Screen for asexual growth on an extensive
134 library of non-clonal *P. berghei* KO parasites, it was posited that the gene is dispensable for
135 the progression of blood-stage parasitemia. Our subsequent analysis of transcription levels
136 by RT-PCR support this, demonstrating that *PDI-Trans* transcripts were present in wild-type
137 asexual erythrocytic stages of gametocyte deficient strain 2.33, in addition to inactive (Gc-)
138 and activated (Gc+) gametocytes, ookinetes and sporozoites (Figure 1A). To investigate the
139 cellular localization of *PDI-Trans* across the parasitic lifecycle targeted-single homologous
140 recombination was utilized to generate a transgenic *P. berghei* parasite expressing the

141 endogenous *PDI-Trans* protein with a C-terminal EGFP fusion tag. Successful integration
142 following drug selection was confirmed by PCR (Figure 1B). The presence of the EGFP tag
143 caused no observable impact on blood or sexual stages, and did not impact transmission
144 through *An. stephensi* mosquitoes. Immunofluorescence microscopy on non-permeabilized
145 parasites confirmed *PDI-Trans*-GFP expression on the surface of activated male gametes and
146 ookinetes (Figure 1C). Live microscopy of mixed blood stages and fixed immunofluorescence
147 of sporozoites demonstrated that *PDI-Trans*-GFP is expressed across the entire parasitic
148 lifecycle (Figure S1).

149

150 ***PDI-Trans* is essential for parasite transmission, is male specific and demonstrates**
151 ***classical PDI activity***

152

153 To investigate the function of *PDI-Trans* targeted gene disruption was used to replace the
154 entire *PDI-Trans* coding sequence. This was performed by double homologous recombination
155 as described in [38,39], with constructs designed and manufactured by Plasmogem (Sanger
156 Institute, UK). Following dilution cloning of drug-resistant parasites, genotyping by PCR of two
157 independently produced clones (Figure 2A) indicates that the replacement construct had
158 integrated at the targeted site, disrupting the endogenous locus. Consistent with previous
159 predictions [37], examination of mice infected with Δ *PDI-Trans* clones showed that the
160 parasites underwent normal asexual development in erythrocytes (Figure S2). Rates of
161 gametocytogenesis and sex ratio were unaffected, and gametocytes were able to emerge
162 from their host cells and differentiate into gametes when exposed to standard gamete
163 activation conditions (i.e. drop in pH or temperature, presence of xanthurenic acid). To
164 examine for a specific role during fertilization we specifically examined *in vitro* ookinete
165 formation in blood collected from mice infected with Δ *PDI-Trans* parasites. Blood cultures from
166 mice infected with Δ *PDI-Trans* parasites failed to produce ookinetes, a finding confirmed by
167 triplicate experiments on two independent Δ *PDI-Trans* clones (Figure 2B). To further explore
168 this phenotype *in vivo*, *An. stephensi* mosquitoes were fed on mice infected with Δ *PDI-Trans*

169 parasites in triplicate, and 12 days later microscopy was used to examine the presence of
170 oocysts (Figure S3). Triplicate experiments of each clone showed a mean reduction of 94.38%
171 inhibition in intensity and 63.68% inhibition in prevalence with in *ΔPDI-Trans* clone 1, and a
172 96.43%/65.62% inhibition in intensity/prevalence with *ΔPDI-Trans* clone 2 when compared to
173 wild type *P. berghei* (Table 1). These results suggest that *Trans-PDI* plays a key role in the
174 successful transmission of *Plasmodium*.

175

176 Cross-fertilization experiments, with known gender-specific sexual mutants, such as the male-
177 deficient *map2* or the female-defective *nek4* mutant [40,41], make it possible to detect gender-
178 specific sterility phenotypes in *P. berghei*. As shown in Figure 2C, neither *Δmap2* nor *Δnek4*
179 strains produce ookinetes when cultured in isolation, but when cultures containing both KO
180 lines were mixed, *Δnek4* male gametes are able to fertilize *map2* female gametes, restoring
181 the capacity to form ookinetes (Figure 2C). Reduced conversion rates (compared with wild
182 type parasites) are expected [3, 40, 41], due to the persistence of *Δnek4* female and *Δmap2*
183 gametes which are unable to fertilize. In *ΔPDI-Trans* /*Δnek4* crosses the *PDI-Trans* female
184 gametes were fertilized by *Δnek4* male gametes, but *Δmap2* females remained unable to
185 differentiate into ookinetes in *ΔPDI-Trans*/*Δmap2* crosses (Figure 2C), indicating that *ΔPDI-*
186 *Trans* males are sterile. Thus, these results demonstrate that during plasmodial fertilization,
187 *PDI-Trans* is essential for microgamete (male) fertility.

188

189 PDI enzymes typically catalyze the rearrangement of disulphide bonds between cysteine
190 residues within proteins. To determine whether *PDI-Trans* exhibits classical PDI activity we
191 utilized a fluorescent PDI insulin-reduction assay to determine reductase activity.
192 Recombinant human PDI was used as a positive control for PDI activity, and the well-
193 characterized PDI inhibitor bacitracin was used as a negative control. Gametocytes from
194 *ΔPDI-Trans*, *ΔPDI-Trans Comp* and wild type lines were purified on a density gradient and
195 used within the assay in either an inactive, or activated form. PDI activity was expressed as a
196 percentage relative to the positive control (Figure 2D). In wild type parasites, PDI activity is

197 increased post-activation, implicating broad PDI activity throughout gamete
198 activation/fertilization. The activated gametes of the ΔPDI -*Trans* line had significantly reduced
199 PDI activity with respect to wild type gametes, specifically indicating that *PDI-Trans* exhibits
200 true PDI reductase function during fertilization. PDI activity was significantly increased when
201 ΔPDI -*Trans* was complemented with the endogenous gene (ΔPDI -*Trans Comp*). To
202 investigate whether complementation restored not only PDI activity, but the ability of these
203 parasites to successfully fertilize we performed ookinete conversion assays. Wild type
204 parasites had a mean conversion rate of 77.98%. Ookinete conversion was not observed in
205 the ΔPDI -*Trans* parasite line. Conversely, ΔPDI -*Trans Comp* parasites exhibited a mean
206 ookinete conversion rate of 72.25% indicating that complementation of the *PDI-Trans* restored
207 the ability to of male gametes to fertilize. Assays were performed in triplicate (Figure 2E).

208

209 ***Malarial transmission is inhibited reversibly by the PDI inhibitor Bacitracin in P. berghei***
210 ***and P. falciparum***

211

212 To further explore *PDI-Trans* activity, and to examine the ability of specific PDI inhibitors to
213 block malarial transmission, we utilized the classical PDI inhibitor bacitracin [42]. The addition
214 of bacitracin during fertilization *in vitro* resulted in a dose-dependent reduction of observable
215 exflagellation centres (motile male and female gametes bound to each other), with a complete
216 inhibition in formation of exflagellation centers at 3 mM (Figure 3A). This subsequently
217 inhibited the ability of mature gametocytes to form ookinetes, with complete inhibition of
218 ookinete conversion at 3 mM bacitracin (Figure 3B). In order to test whether bacitracin has a
219 broad and non-specific toxic effect on parasites, potentially unrelated to *PDI-Trans* function,
220 gametocytes were pre-incubated in bacitracin at a range of concentrations for 30 minutes,
221 washed to remove the PDI inhibitor, then assayed for formation of exflagellation
222 centers/ookinetes respectively (post-wash). Results show that parasites pre-incubated with
223 bacitracin, then washed, resulted in no significant difference (Paired t test) in the number of

224 exflagellation centres compared to the untreated control across all concentrations examined
225 (Figure 3C-D).

226

227 In an attempt to further examine the activity of *PDI-Trans* and the mechanism of PDI-inhibitor
228 based blockade of transmission, following bacitracin treatment we examined the number of
229 visible free floating male gametes present, compared with the number of exflagellation centers
230 present (defined as three or more male gametes adhered to a female gamete). As bacitracin
231 concentrations increased. the number of visible exflagellation centres decreased, conversely,
232 the number of free floating observed microgametes was unaffected (Figure 3E), suggesting
233 that PDI activity is essential for the association of male and female gamete to form
234 exflagellation centers, but not for the ability of gametogenesis/activation to form
235 microgametes.

236

237 To test the ability of bacitracin to block the transmission of *P. berghei ex vivo* we performed
238 standard membrane feeding assays (SMFA) in triplicate with 0.3, 1 and 3 mM doses of
239 bacitracin (Figure 3 F-H). Bacitracin inhibited transmission at all concentrations in a dose-
240 dependent manner with a maximal inhibition in oocyst intensity of 98.21% and infection
241 prevalence of 92.48% with 3 mM bacitracin (Table 2).

242

243 To investigate if PDI function is implicated in fertilization in additional *Plasmodium* species,
244 and to extend our observations in *P. berghei* to human malaria parasites, we performed
245 SMFAs with *P. falciparum* gametocyte cultures in the presence of bacitracin. Given the results
246 observed with *P. berghei* we chose to perform the *P. falciparum* feeds at the highest
247 concentration of bacitracin (3 mM) in triplicate to detect maximal effect (Figure 3 I-K). The
248 addition of bacitracin significantly inhibited transmission, with a mean inhibition in oocyst
249 intensity of 95.05% and an inhibition of oocyst prevalence of 81.71% observed (Table 3).

250

251 ***PDI-Trans can be targeted specifically with antibodies to block transmission in vitro***
252 ***and ex vivo***

253

254 Considering the surface localization of *PDI-Trans* on the surface of the microgamete and
255 ookinete, the ability of anti-*PDI-Trans* antibodies to initiate a specific anti-parasitic
256 transmission blocking response was additionally examined. A polyclonal peptide antibody
257 raised against residues bioinformatically predicted to be within the extracellular domain of *PDI-*
258 *Trans* (amino acids 30 - 43). Antibodies were raised in rabbits, IgG purified, and examined for
259 their ability to inhibit transmission *in vitro* and *ex vivo*. Anti-*PDI-Trans* IgG recognized both
260 non-permablized gametocyte and ookinetes by IFA (Figure 4A). Staining was absent in
261 secondary only controls, indicating the ability of these antibodies to specifically recognize
262 natively folded *PDI-Trans* on the gamete and ookinete surface (Figure 4B).

263

264 To examine the ability of *PDI-Trans* to act a transmission blocking antigen, we performed *in*
265 *vitro* ookinete conversion assays in the presence of anti-*PDI-Trans*. Anti-*PDI-Trans* inhibited
266 ookinete conversion in a dose-dependent manner, further suggesting specificity. At antibody
267 concentrations of 50, 100, 250 and 500 µg/ml, ookinete formation was inhibited by 14.3%,
268 33.2%, 38.7% and 75.4% respectively. In contrast, as previously demonstrated [4], the
269 presence of UPC10 (negative control) had no effect on ookinete conversion (Figure 4C).

270 The transmission blocking activity of anti-*PDI-Trans* antibodies were additionally assessed by
271 triplicate SMFA (Figure 4D-F). Given the *in vitro* results observed previously (Figure 4D), we
272 assessed the *in vivo* transmission blocking ability of these antibodies only at the highest
273 concentration where an effect in the *in vitro* ookinete assay was demonstrated. Anti-*PDI-Trans*
274 antibodies significantly inhibited *P. berghei* transmission in all experiments. At a concentration
275 of 500 µg/ml anti-*PDI-Trans* antibodies inhibited oocyst intensity by a mean of 66.22% and
276 reduced prevalence of infection by 33.16% (Table 4).

277

278 **Discussion:**

279

280 Fertilization is a key process in the *Plasmodium* lifecycle, encompassing the active fusion of
281 activated male (micro) and female (macro) gametes to form a zygote within the mosquito
282 bloodmeal. The resulting diploid zygote develops into a motile ookinete, establishing infection
283 in the mosquito midgut and further progression throughout the Anopheline host. Despite its
284 essential nature to the success of the parasitic lifecycle, the cellular and molecular
285 mechanisms that underlie gamete fertilization of male and female gametes remain largely
286 opaque in *Plasmodium* (and for the majority of Apicomplexa). Gamete interaction is a two-
287 phase process; in the first phase, cell adhesion molecules displayed on the surfaces of the
288 male and female gametes are responsible for gamete-gamete recognition. This initial
289 recognition/adhesion step initiates a signal transduction cascade that activates the sperm and
290 exposes new, fusogenic regions of the sperm plasma membrane. In *Plasmodium*, only three
291 proteins have been discovered that have a demonstrable role in the mutual recognition of
292 gametes; the 6-Cys family members, P48/45, P47 and P230 [5]. The specific mechanism of
293 action of these proteins are currently unknown. In the absence of many of these surface
294 proteins, there is a significant reduction in the formation of zygotes, however, low levels of
295 fertilization still occur, particularly *in vitro* [3,6,7], indicating that gametes potentially use
296 alternative, currently unknown, molecules to recognize each other. In the second phase of
297 fertilization, the plasma membranes of the two gametes come into intimate contact and then
298 fuse, bringing about cytoplasmic continuity. The conserved class II fusion transmembrane
299 protein HAP2 is essential for gamete fusion during fertilization, and initiates merger of lipid
300 bilayers post gamete adhesion. Following a (currently uncharacterized) trigger, it is
301 hypothesized that a short-conserved region within the *Plasmodium* HAP2 ectodomain
302 becomes exposed on the microgamete membrane surface, leading to the alignment of protein
303 subunits parallel to each other, favoring trimerization [4,43,44]. Polar residues on the fusion
304 loop are subsequently inserted into the target (macrogamete) membrane, followed by a
305 conformational change in HAP2 domain III which distorts the target membrane, leading to

306 hemifusion and then fusion/cytoplasmic continuity. Further related upstream and downstream
307 effector molecules that specifically mediate the process of fertilization are at present unclear.

308

309 Here, we demonstrate that protein disulphide isomerase function, specifically encoded by a
310 single plasmodial gene (*PDI-Trans*/PBANKA_0820300) is essential for malarial transmission.

311 We demonstrate that *PDI-Trans* is constitutively expressed throughout the parasitic lifecycle,

312 in both the blood and mosquito stages, but is only essential in the male gamete, where it is

313 surface expressed. Absence of *PDI-Trans* only confers a detectable effect post-gamete

314 activation, prior to gamete adhesion, and is null for male fertility, and consequently,

315 zygote/ookinete formation, and transmission to the mosquito host. Complementation of the

316 disrupted locus restores fertility. Furthermore, we conclusively demonstrate specific reductase

317 activity, indicative of “classical” PDI activity, Inhibition of *PDI-Trans* using the widely available

318 (topical) antibiotic and PDI inhibitor, bacitracin, reversibly blocks plasmodial transmission *in*

319 *vivo* and *ex vivo*. Specifically, the process of gamete activation remains unaffected by

320 bacitracin, whereas the ability of treated gametes to adhere to other cells (i.e. form

321 exflagellation centers) appears to be compromised. Bacitracin-derived transmission blockade

322 is observed in both *P. berghei* and *P. falciparum*. Finally, we show that antibodies specifically

323 raised against the extracellular region of *PDI-Trans* can recognize the surface of the sexual

324 stages of the parasite by immunofluorescence, and can initiate transmission-blocking activity

325 both *in vitro* and *ex vivo*.

326

327 In all living cells, the appropriate formation and cleavage of disulphide bonds between cysteine

328 residues in secreted and membrane-anchored proteins is essential for native conformation,

329 and therefore, function. PDIs are traditionally known to be versatile enzymes with key roles in

330 the mediation of disulfide bond formation, isomeration and reduction in the endoplasmic

331 reticulum [32]. PDI function is also associated with varied chaperone activity [31]. Little is

332 known regarding the expression and function of PDI-like proteins in *Plasmodium*. A previous

333 study [33] has bioinformatically identified nine PDI-like molecules across five species of

334 malaria parasites (four in *falciparum*, one in *vivax*, *berghei*, *knowlesi* and *yoelii*), indicated by
335 the presence of classical thioredoxin domains. A more detailed analysis of one of these PDI
336 candidates in *P. falciparum*; PfPDI-8 (PF3D7_0827900), demonstrated expression within the
337 endoplasmic reticulum of asexual blood schizonts, gametocytes and sporozoites, with
338 biochemical analysis indicating a function in the disulfide-dependent conformational folding of
339 a recombinant form of the erythrocyte-binding protein (and putative bloodstage vaccine target)
340 EBA-175. As further evidence of the chaperone function of PDI enzymes, studies utilizing the
341 overexpression of PfPDI-8 resulted in the enhanced expression and folding of the
342 transmission-locking vaccine candidate, Pf25, in a *Pichia pastoris* expression system [59].
343 Broadly, PDI function is bioinformatically predicted to be conferred by multiple ORF throughout
344 the parasitic genome. Expression, localization and function of these proteins are still largely
345 undefined. Future study to further dissect the function of PDIs (and associated mechanisms
346 of protein folding) in *Plasmodium* may be advantageous.

347

348 Although classically considered to be key mediators of protein folding in the endoplasmic
349 reticulum, key evidence showing localization and function of PDIs in other cell compartments
350 does exist. In some organisms, PDIs have been demonstrated to on occasion escape the ER,
351 and exhibit cytoplasmic and cell surface localization, where their predominant function
352 appears to be the reduction of disulphide bonds [32,45]. In terms of fertilization, PDI activity
353 on the sperm head has previously proved to be essential for sperm-egg cell fusion in multiple
354 vertebrates [31,46-48], and implicated in male fertility in mice [49,50]. PDI function has
355 previously been implicated in the progression of multiple infectious diseases, with a specific
356 role in mediating pathogen entry. In viruses, overexpression of PDI enhances the fusion of viral
357 membranes, leading to increased internalization of HIV-1 [51]. Cell surface PDI has been
358 shown to facilitate the infection of HeLa cells by mouse polyoma virus [52], and in endothelial
359 cells a surface localized (lipid-raft associated) PDI reduces $\beta 1$ and $\beta 2$ integrins, allowing for
360 the entry of dengue virus [53,54]. Its function is also essential for release of cholera toxin active
361 chain A from the ER to the cytosol of the infected cell [54,55]. In protozoan pathogens,

362 previous experimentation has demonstrated that increased levels of PDI increase the
363 phagocytosis of the *L. chagasi* promastigote (but not the amastigote) [56]. It has previously
364 been hypothesized that *T. gondii* and *L. donovani* PDI could be putative targets for vaccine
365 development [57,58]. The specific function of *PDI-Trans* within the parasite is still unknown,
366 however, it is clear that the process of successful fertilization in *Plasmodium* requires the
367 presence and function of a range of proteins with conserved disulphide bonds between
368 cysteine residues on the gamete surface. The 6-Cys family members P48/45, P47, P230 are
369 all definitively evidenced to mediate gamete adhesion, whereas HAP2 requires the correct
370 formation of multiple crucial disulphide bridges to enable membrane fusion. It cannot be
371 discounted that *PDI-Trans* may in some way catalyse disulphide bond rearrangement in one
372 of these transmission-essential proteins, exposing key residues critical for fertility-based
373 function. Given the ability of the *PDI-Trans* knockout described here to undergo normal levels
374 of gametogenesis, function post-activation, but pre-gamete fusion seems likely.

375

376 The results described here clearly indicate that *PDI-Trans* is a potential target for anti-malarial
377 compounds or vaccines to successfully inhibit malarial transmission. The generation of novel
378 TBIs to reduce disease burden is a key component of the current anti-malarial strategy, and it
379 is widely accepted that to achieve eradication, it will be necessary to use interventions that
380 inhibit the transmission of parasites from humans to mosquitoes [2]. We demonstrate that
381 bacitracin reversibly inhibits malarial transmission with high efficacy, and additionally, that
382 antibodies targeting *PDI-Trans* on the surface of the sexual stages of the parasite mediate
383 significant transmission blocking immunity. It should be noted that bacitracin is already an FDA
384 approved compound, traditionally used clinically against gram-positive compounds. This
385 example illustrates the potential value of re-purposing drugs with observed efficacy against
386 non-malarial species. Previous studies examining the anti-malarial efficacy of bacitracin only
387 examined impact on asexual growth, where no effect was demonstrated [64]. The data here
388 provides further evidence that potent anti-malarial transmission blocking efficacy can be
389 achieved by targeting the male (micro) gamete. Previously described compounds effective

390 against the process of fertilization (methylene blue and atovaquone) are effective in blocking
391 transmission, as are antibodies against multiple male gamete-surface proteins [21-27]. To
392 target the sexual stages of the malaria parasite further, a deeper understanding of
393 transmission and specifically, the mechanism of fertilization within *Plasmodium* is
394 advantageous, and offers the potential for the development of new, effective interventions.
395 More broadly, PDI-like proteins are expressed across multiple taxa, and species, including in
396 a wide range of organisms of veterinary and clinical importance [31,46]. Given the ability of
397 both anti-*PDI-Trans* compounds and antibodies to block malarial transmission described here,
398 and the proven role of PDI function in the regulation of infection across multiple species, it is
399 not unreasonable to suggest that further studies may want to examine the possibility of
400 targeting PDI proteins/functions using specifically designed novel anti-malarial drugs or
401 vaccines.

402

403 **Experimental procedures:**

404 ***General parasite maintenance***

405 General parasite maintenance was carried out as described in [60]. Briefly, *P. berghei*
406 parasites were maintained in 6–8-week-old female Tuck Ordinary (TO) mice (Harlan) by serial
407 mechanical passage (up to a maximum of eight passages). If required, hyper-reticulosis was
408 induced three days before infection by treating mice intraperitoneally (*i.p.*) with 200 μ l
409 phenylhydrazinium chloride (PH; 6 mg/ml in PBS; ProLabo UK). Mice were infected *i.p.* and
410 infections were monitored using Giemsa-stained tail blood smears as described previously
411 [70].

412

413 ***Generation and analysis of transgenic parasite lines***

414 *PDI-Trans-GFP*

415 To examine the expression and localization of *PDI-Trans*, the *PDI-Trans-GFP* transgenic line
416 was created, introducing a C-terminal GFP tag to the native by single homologous
417 recombination. The targeting construct *pPDI-Trans-GFP* was constructed using the backbone

418 of the EGFP-tagging vector p277 [62]. The terminal 1527 bp of the *PDI* gene
419 (PBANKA_082030) was synthesized (IDT) to remove internal *ApaI* site and introduce unique
420 *AvrII* site within the gene and flanking *KpnI* and *ApaI* sites to the amplicon. This block was
421 cloned in frame into *Apal/KpnI* sites of p277, resulting in *pPDI-Trans -GFP*. For transfection,
422 this construct was linearized at a unique *AvrII* site within the *PDI* sequence.

423 Parasites were transfected using the Nucleofector device (Amaxa Biosystems) as described
424 previously [62]. Integration of the DNA constructs into the chromosome was confirmed by PCR
425 flanking a region upstream from the 5' integration site into the EGFP sequence (oligo 35; 5'-
426 GCATGTGCGATTGTATTGGG-3; oligo 14; 5'-ACGCTGAACTTGTGGCCG-3') and the
427 presence of the DHFR selection cassette (oligo 91 5'- TTCGCTAAACTGCATCGT -3'; oligo
428 92 5'-GTACTIONAATGCCTTTCTCCT-3'). Oligos against the *Pbs25* gene (PBANKA_0051500)
429 were used as positive control (oligos F1: 5'-
430 CAACTTAGCATAAATAATAATAATGCGAAAGTTACCGTGG-3'; F2 5'-
431 CCATCTTTACAATCACATTTATAAATTCCATC-3'). GFP expression in transfected, drug
432 resistant parasites were confirmed by fluorescence microscopy. Two independent clones were
433 obtained from two independent transfections, demonstrating identical phenotypes and GFP
434 expression.

435 *ΔPDI-Trans*

436 To examine the function of PBANKA_082030 the *ΔPDI-Trans* transgenic line was generated.
437 The plasmid was designed and constructed by PlasmogEM (PlasmogEM ID PbGEM-239637)
438 using recombinase-mediated engineering followed by a Gateway® mediated exchange
439 [39,63]. Prior to transfection the construct was digested by *NotI* to release the *P. berghei*
440 insert from its vector backbone. Parasites were transfected using the Nucleofector device
441 (Amaxa Biosystems) as described previously [62]. Integration of the DNA constructs into the
442 chromosome was confirmed by PCR region flanking 5' of the modified target locus and 3'
443 DHFR selection cassette (oligo 72; 5'- ACGTGCATGTGCGATTGTATTGGGT -3; oligo 9; 5'-

444 CTTTGGTGACAGATACTAC -3') and the absence of the wildtype locus (oligo 69 5'-
445 ATGGGAAACTATACTTATATATATATATTTTTTTTCA -3'; oligo 70 5'-
446 TTATAAATCAGAATTTTCTTCTCCTTC -3'). Two independent clones were obtained from two
447 independent transfections, demonstrating statistically indistinguishable phenotypes.

448 *ΔPDI-Trans-Comp*

449 For the complementation construct the clonal knockout line was injected into mice and mice
450 were treated with 5-Fluorocytosine (5FC) nucleoside analog (Sigma) drinking water, 1.5 mg/ml
451 to recycle the *Hdhfr-yfcu* marker. The subsequent marker free line was subjected to dilution
452 cloning to achieve a pure population of marker free parasites. Following this the full length
453 endogenous PBANKA_082030 gene was transfected on top using the artificial chromosome
454 library clone mapping to PBANKA_082030 from PlasmoGEM (clone ID PbAC02-74d11) as
455 described previously (Figure S4) [37, 62].

456

457 **RT-PCR**

458 *P. berghei* RNA was isolated from gametocyte deficient strain 2.33, activated or inactivated
459 gametocytes, ookinetes and sporozoites from wild type *P. berghei* 2.34 strain using Trizol
460 reagent (Invitrogen). cDNA synthesis was performed using Prime script kit from (Clonetechn).
461 PCR reactions were set up to amplify sections of *PDI-Trans* ORF (Forward 5'-
462 ATGGGAAACTATACTTATATATATATATTTTTTTTCA-3'; and reverse 5'-
463 CTACATATTTATCGACATCTCCAA-3'). The expected RT amplicon was 481 bp. The
464 ubiquitously expressed α -tubulin gene PB300720.00.0 was amplified for each sample to
465 ensure amplifiability of cDNA from respective RNA samples (Forward, 5'-
466 CCAGATGGTCAAATGCCC-3'; Reverse, 5'-CTGTGGTGATGGCCATGAAC-3'). The
467 expected products were 435 bp (cDNA). Thirty RT-PCR cycles were carried out with
468 denaturation for 1 min at 94°C, annealing for 45 secs at 50°C, and extension for 1.5 min at
469 68°C, and products were visualized on a 0.8% agarose gel.

470

471 **Direct Feeding Assay (DFA)**

472 Routine maintenance of *P. berghei* was carried out as described above. Prior to challenge,
473 mice were PH treated, and 3 days later infected *i.p.* with 10^6 *P. berghei* ANKA 2.34 or Δ *PDI-Trans*
474 parasites. Three-days post-infection, animals were anesthetized, and >50 female
475 *Anopheles stephensi* mosquitoes allowed to blood feed on each mouse. Twenty-four hours
476 later, unfed mosquitoes were removed. Mosquitoes were maintained on 8% (w/v) fructose,
477 0.05% (w/v) p-aminobenzoic acid at 19-22 °C and 50-80% relative humidity. Day 14 post-
478 feeding, mosquito midguts were dissected and oocyst intensity and prevalence observed by
479 standard phase microscopy and recorded. Reduction in oocyst intensity and prevalence in
480 knockout mice were calculated with respect to wild type controls.

481

482 **In Vitro Ookinete Conversion Assay (IVOA)**

483 PH-treated mice were injected with 5×10^7 parasites *i.p.* On day 3 or 4 of infection, parasitaemia
484 was counted on a Giemsa- stained tail blood smear and exflagellation of male gametocytes
485 was checked by addition of a drop of exflagellation medium to a drop of tail blood. Hosts
486 observed to have exflagellating parasites were exsanguinated by cardiac puncture and each
487 20 μ l of blood taken up in 450 μ l ookinete medium. Individual cultures were then added to pre-
488 prepared 24 well plates (Nunc) and incubated for 24h at 19°C. Cultures were harvested after
489 24h by centrifugation (500 \times g, 5min), washed once in 100 μ l ookinete medium, and the pellet
490 taken up in 50 μ l ookinete medium containing Cy3-conjugated Pbs28 mAb clone 13.1 (1:500).
491 Ookinetes and macrogametocytes were then immediately counted by fluorescence
492 microscopy. Ookinete conversion rates were calculated as described previously [19]. In
493 bacitracin experiments harvested parasites were added to ookinete medium containing a
494 range of Bacitracin (Sigma Aldrich: #B0125) concentrations and either left in or washed and
495 put into fresh medium 30 min after drug treatment. In antibody experiments harvested
496 parasites were added to ookinete medium containing anti-*PDI-Trans* rabbit sera or anti-

497 UPC10 (negative control). In each set of experiments results were collated from three separate
498 experiments and inhibition expressed as the percentage reduction in ookinete conversion with
499 respect to wild type parasites, samples with no bacitracin or the anti-UPC10 control.

500

501 **Crosses**

502 At day 3 post infection of phenylhydrazine treated mice, infected with parasites with either
503 $\Delta PDI-Trans$, $\Delta nek4$, $\Delta map2$ and wt were harvested by heart puncture and mixed at a 1:1 ratio
504 in ookinete medium. After 24 h, ookinete conversion assays were performed by incubating
505 samples with 13.1 antibody (antibody against Pb28 conjugated with Cy3). The proportion of
506 ookinetes to all 13.1-positive cells (unfertilised macrogametes and ookinetes) was
507 established, counting fields at 60 × magnification. Experiments were performed in biological
508 triplicate [40,41].

509

510 **PDI activity assay**

511 PDI activity was measured in a microplate PDI inhibitor screening assay kit from Abcam
512 (ab139480). Briefly, $\Delta PDI-Trans$ $\Delta PDI-Trans$ Comp and wild-type gametocytes were purified
513 [72]. Both activated and non-activated gametocytes of each parasite line were used in the
514 assay and the PDI-catalyzed reduction of insulin in the presence of Dithiothreitol resulting in
515 the formation of insulin aggregates which bind avidly to the red-emitting fluorogenic PDI
516 detection reagent were measured on Tecan, Infinite M200 Pro. The background media signal
517 for each sample was subtracted and PDI activity was calculated as a percent relative to the
518 positive control (human recombinant PDI). Experiments were performed in triplicate.

519

520 **Standard Membrane Feeding Assay (SMFA)**

521 *P. berghei*

522 Female *An. stephensi* (SDA 500 strain) were starved for twenty-four hours and then fed on
523 heparinized *P. berghei* infected blood using standard membrane feeding methods [60]. For
524 each feed, 350 μ l of *P. berghei* ANKA 2.34 infected blood containing asexual and sexual

525 stages of the parasite was mixed with 150 μ l of PBS containing either antibody to yield final
526 concentration of 500 μ g/ml or drug at 0.3, 1 and 3 mM. Mosquitoes were handled, maintained
527 and analyzed as described above. Reductions in oocyst intensity and prevalence was
528 calculated with respect to control feeds as described in [4].

529

530 *P. falciparum*

531 Mature gametocytes of *P. falciparum* (NF54) were produced *in vitro* as described previously
532 [65] with slight modifications. Briefly, mature gametocyte cultures (0.5 to 2 % final
533 gametocytaemia) were fed for 15-20 min at room temperature to *An. gambiae* mosquitoes
534 through an artificial membrane kept at 37 °C. For each feed 300 μ l of mature *P. falciparum*
535 gametocytes were mixed with bacitracin at a concentration of 3 mM. Engorged mosquitoes
536 were housed in pots at 26°C and 60–80% relative humidity. On days 7-9, midguts were
537 dissected and the results analyzed as outlined in the above *P. berghei* section.

538

539 **Antibody production**

540 Synthetic peptide to *PDI-Trans* (VSDDFAKKVNHLTHC) was produced, conjugated to KLH
541 and used to raise polyclonal rabbit antisera (Genscript, USA). Resulting sera was IgG purified
542 and validated by Genscript via ELISA.

543

544 **Microscopy:**

545 *Immunofluorescence assay (IFA)*

546 *PDI-Trans*-GFP parasites were assessed by IFA for the presence of GFP tag with anti-GFP,
547 Roche at a dilution of 1:500. Signal was detected by Alexa Fluor 488-labelled goat, anti-mouse
548 IgG (Molecular Probes) at 1:500. Rabbit antibodies to *PDI-Trans* were assessed by IFA on
549 wild-type *P. berghei* ANKA 2.34 gametocytes and ookinetes at a dilution of 1:500. Signal was
550 detected by Alexa Fluor 488-labelled goat, anti-rabbit IgG (Molecular Probes) at 1:500.
551 Parasites were cultured and IFAs were performed as described previously [4]. Slides were

552 visualized under x60 objective magnification using a fluorescence microscope (EVOSFL Cell
553 Imaging System, Life Technologies).

554 *Live imaging*

555 *PDI-Trans-GFP* parasites were examined for GFP signal by live microscopy. Parasites were
556 cultured and allowed to settle on glass slides before microscopy. Slides were visualized under
557 X40 objective magnification using a fluorescence microscope (Leica DMR).

558

559 **Statistical Analysis**

560 Statistical analysis was performed using Graphpad Prism. For DFA, SMFA and DMFA,
561 significance was assessed using Mann–Whitney U (to examine differences in intensity) and
562 Fisher's exact probability tests (to examine differences in prevalence). Parametric ELISA tests
563 were assessed using t-test. P values < 0.05 were considered statistically significant (*** =
564 <0.0001, ** = 0.001, * = 0.001-0.01, = 0.01-0.05).

565

566 **Ethical Statement**

567 All procedures were performed in accordance with the UK Animals (Scientific Procedures) Act
568 (PPL 70/8788) and approved by the Imperial College AWERB. The Office of Laboratory
569 Animal Welfare Assurance for Imperial College covers all Public Health Service supported
570 activities involving live vertebrates in the US (no. A5634-01).

571

572 **Acknowledgements:**

573 This work was funded by the MRC (New Investigator Research Grant; award number
574 MR/N00227X/1) A.M.B thanks PATH-MVI for funding. Funders had no role in study design,
575 data collection and interpretation, of the decision to submit the work for publication. We
576 gratefully acknowledge Mark Tunnicliff for mosquito production and Tibebe Habtewold for
577 advice regarding *P. falciparum* infections.

578

579 **Conflicts of Interest:**

580 The authors are not aware of any conflicts of interest arising from this work.

581 **Figure Legends:**

582 **Figure 1. Constitutive expression of *Plasmodium berghei* PDI-Trans, and localization**

583 **on the surface of gametocytes and ookinetes. A).** RT-PCR analysis of *PDI-Trans* in

584 asexual blood stages using the non-gametocyte producing strain 2.33; non-activated (Gc-)

585 and activated (Gc+) gametocytes; purified *in vitro* ookinetes and day 21 salivary gland

586 dissected sporozoites. The analysis was complemented with alpha-tubulin loading controls

587 **B).** PCR confirmation of integration of *egfp* into the *PDI-Trans* locus. Oligonucleotides 35 and

588 14 were used to detect integration. Oligonucleotide 91 and 92 were used to detect DHFR

589 presence, *pbs25* oligonucleotides were used as positive controls. *P. berghei* WT 2.34 gDNA

590 was used as a negative control for integration. **C).** IFA of fixed, non-permeabilised *PDI-Trans-*

591 *GFP* parasites probed with anti-GFP; exflagellating male gametocytes (top) and ookinetes

592 (bottom). Each panel shows an overlay of GFP fluorescence (green) and DNA labelled with

593 DAPI (blue). White scale bar = 5 μ m.

594

595

596 **Figure 2. Deletion of *PDI-Trans* strongly inhibits transmission and is male specific**

597 **A).** Diagnostic PCR with genomic DNA templates and primers 69 and 70 to test for the

598 presence of *PDI-Trans*, and primers 72 and 9 to detect a unique 930bp product across the

599 integrations site. **B).** The bar chart shows ookinete conversion rates for wild type and both

600 Δ *PDI-Trans* clones. Conversion rate is expressed as a percentage of P28-positive parasites

601 that had progressed to the ookinete stage (error bar indicates SEM; $n=3$). Asterisks indicate

602 P value < 0.05 Paired t test **C).** *In vitro* ookinete conversion analysis demonstrates that *PDI-*

603 *Trans* mutant shows production cross-fertilisation with the Δ *nek4* sterility mutant, which

604 produces functional males only, and not with Δ *map2* mutant, which produces functional

605 females only. (error bar indicates SEM; $n=3$). Asterisks indicate P value < 0.05 Paired t test.

606 **D).** PDI activity of purified active and inactive gametocytes from wild type, Δ *PDI-Trans* and

607 Δ *PDI-Trans* Comp parasite lines. PDI activity is expressed as a percent relative to the positive

608 control (human recombinant PDI). Experiments were performed in triplicate (error bar
609 indicates SEM; $n=3$). Asterisks indicate P value < 0.05 Paired t test. **E**). Bar chart of ookinete
610 conversion rates for wild type $\Delta PDI-Trans$ and $\Delta PDI-Trans$ Comp parasite lines. Conversion
611 rate is expressed as a percentage of P28-positive parasites that had progressed to the
612 ookinete stage (error bar indicates SEM; $n=3$). Asterisks indicate P value < 0.05 Paired t test
613

614 **Table 1. Mean *in vivo* evaluation of deleting *PDI-Trans* on transmission by direct**
615 **feeding.**

616 The mean (from three replicates) inhibition in intensity (mean number of oocysts per midgut)
617 and prevalence of two independent *PDI-Trans* knockout clones were calculated with respect
618 to wild type controls. ^a P < 0.05, Mann-Whitney U test ^b P < 0.05, Fisher's exact test.

619

620 **Figure 3. The specific PDI inhibitor bacitracin reversibly inhibits *Plasmodium berghei***
621 **fertilization *in vivo* and transmission *ex vivo*.**

622 **A**). Exflagellation centers in the presence of Bacitracin at 0, 0.03, 0.3, 1 mM. Asterisks indicate
623 P value < 0.05 Paired t test. **B**). *In vitro* ookinete development assay supplemented with
624 Bacitracin at 0, 0.03, 0.3, 1 and 3 mM. Results are shown as percent inhibition in ookinete
625 conversion. Asterisks indicate P value < 0.05 Paired t test, ns indicate P value not significant.

626 **C**). Exflagellation centers after 30 minutes in the presence of Bacitracin at 0, 0.03, 0.3, 1. P
627 value < 0.05 Paired t test indicates P value not significant at any concentration. **D**). *In vitro*
628 ookinete development assay supplemented with Bacitracin at 0, 0.03, 0.3, 1 and 3 mM for 30
629 min prior to removal of Bacitracin. Results are shown as percent inhibition in ookinete
630 conversion. P value < 0.05 Paired t test indicates P value not significant at any concentration.

631 **E**). Triplicate counts of free floating male gametes and male gametes in exflagellation centers.
632 Represented as a percentage of total events observed in the presence of 0, 0.3, 1 and 3 mM
633 Bacitracin. **F-H**). Triplicate *P. berghei* standard membrane feeding assays with Bacitracin
634 compared to control at concentrations of 0.3, 1 and 3 mM. Individual data points represent the

635 number of oocysts found in individual mosquitoes 12-days post feed. Horizontal bars indicate
636 mean intensity of infection, whilst error bars indicate S.E.M within individual samples. Asterisks
637 indicate P value <0.05 Mann-Whitney *U* test, ns indicate P value not significant. **I-J**). Triplicate
638 *P. falciparum* standard membrane feeding assays with Bacitracin compared to control at a
639 concentration of 3 mM. Individual data points represent the number of oocysts found in
640 individual mosquitoes 8-days post feed. Horizontal bars indicate mean intensity of infection,
641 whilst error bars indicate S.E.M within individual samples. Asterisks indicate P value <0.05
642 Mann-Whitney *U* test.

643

644 **Table 2. Overall evaluation of transmission blocking effect of PDI inhibitor bacitracin in**
645 ***P. berghei* by SMFA.**

646 Mean (from three replicates) reductions in intensity (mean number of oocysts per midgut) and
647 prevalence with bacitracin at 0.3, 1 and 3 mM were calculated with respect to control feeds. ^a
648 P < 0.05, Mann-Whitney *U* test ^b P < 0.05, Fisher's exact test.

649

650 **Table 3. Mean ex vivo evaluation of transmission blocking effect of PDI inhibitor**
651 **bacitracin in *P. falciparum***

652 The mean (from three replicates) changes in intensity (mean number of oocysts per midgut)
653 and prevalence with Bacitracin at 3 mM were calculated with respect to control feeds. ^a P <
654 0.05, Mann-Whitney *U* test ^b P < 0.05, Fisher's exact test.

655

656 **Figure 4. Anti-PDI-Trans antibodies inhibit fertilization and transmission in *Plasmodium***
657 ***berghei*.**

658 IFA of WT *P. berghei* ANKA male gametes and ookinetes with **A**). anti *PDI-Trans* and **B**).
659 Secondary-only control antibodies (green) DAPI (blue). IFA of male gametes and ookinetes
660 with anti *PDI-Trans* shows broad surface staining. White scale bars = 5 μ m **C**). Inhibition in
661 ookinete conversion in *in vitro* ookinete development assay with anti *PDI-Trans* antibody

662 compared to negative control antibody UPC10 at concentrations of 0, 50, 100, 250 and 500
663 µg/ml. Asterisks indicate P value < 0.05 Paired t test, ns indicate P value not significant. **D-F**).
664 Triplicate standard membrane feeding assays with anti *PDI-Trans* antibody compared with
665 negative control antibody UPC10 at a concentration of 500 µg/ml. Individual data points
666 represent the number of oocysts found in individual mosquitoes 12-days post feed. Horizontal
667 bars indicate mean intensity of infection, whilst error bars indicate S.E.M within individual
668 samples. Asterisks indicate P value <0.05 Mann-Whitney *U* test, ns indicate P value not
669 significant.

670

671 **Table 4. Mean ex vivo evaluation of transmission blocking effect of anti-*PDI-Trans***
672 **antibodies**

673 The mean (from three replicates) change in intensity (mean number of oocysts per midgut)
674 and prevalence with anti *PDI-Trans* antibody at 500 µg/ml were calculated with respect to
675 appropriate negative control antibody UPC10 at the same concentration. ^a P < 0.05, Mann-
676 Whitney *U* test ^b P < 0.05, Fisher's exact test

677

678 **Supplemental Figure S1.**

679 **A).** Live GFP fluorescence of mixed blood stage *P. berghei* *PDI-Trans-GFP* parasites. Scale
680 bar = 15 μ m. **B).** IFA of fixed, non-permeabilised *PDI-Trans-GFP* salivary gland sporozoites
681 probed with either anti-GFP (top) or secondary only (bottom). Each panel shows an overlay
682 of GFP fluorescence (green) and DNA labelled with DAPI (blue). Scale bar = 5 μ m.

683

684 **Supplemental Figure S2.**

685 **A).** Asexual growth and **B).** gametocyte production of WT and Δ *PDI-Trans* parasites strains.
686 Three independent experiments are plotted.

687

688 **Supplemental Figure S3.**

689 Mice infected with **A).** Δ *PDI-Trans* clone 1 (C1) or **B).** Δ *PDI-Trans* clone 2 (C2) *P. berghei*
690 parasites and DFA performed to determine transmission blockade. Individual data points
691 represent the number of oocysts found in individual mosquitoes 12 days post feeding.
692 Horizontal bars indicate mean intensity of infection, while error bars indicate SEM within
693 individual samples. Asterisks indicate P value < 0.05 Mann-Whitney U test.

694

695 **Supplemental Figure S4**

696 **A).** Genotyping data for Δ *PDI-Trans*, Δ *PDI-Trans* marker-free and Δ *PDI-Trans* Comp lines.
697 **B).** Schematic of for Δ *PDI-Trans*, Δ *PDI-Trans* marker-free and Δ *PDI-Trans* Comp lines and
698 primer pairs used for genotyping.

699

700 **References:**

701

702 1). World Health Organization W. World Malaria Report (2017).

703

- 704 2). Rabinovich RN, Drakeley C, Djimde AA, Hall BF, Hay SI, Hemingway J, et al. malERA:
705 An updated research agenda for malaria elimination and eradication. *PLoS Med* (2017)
706 14(11): e1002456.
- 707
- 708 3). Liu, Y., Tewari, R., Ning, J., Blagborough, A.M., Garbom, S., Pei, J., Grishin, N.V.,
709 Steele, R.E., Sinden, R.E., Snell, W.J., Billker O. The conserved plant sterility gene HAP2
710 functions after attachment of fusogenic membranes in *Chlamydomonas* and *Plasmodium*
711 gametes. (2008). *Genes and Development* 22, 1051-1068.
- 712
- 713 4). Angrisano F, A. Sala KA, Da DF, Liu Y, Pei J,. Grishin NV. Snell WJ, Blagborough AM.
714 Targeting the Conserved Fusion Loop of HAP2 Inhibits the Transmission of *Plasmodium*
715 *berghei* and *falciparum*. *Cell Reports*. (2017). 21 (10): 2868-2878.
- 716 5). van Dijk MR, van Schaijk BC,. Khan SM, van Dooren MW, Ramesa Jr J, Kaczanowski S,
717 van Gemert GJ, Kroeze H, Stunnenberg HG, Eling WM, et al. Three members of the 6-cys
718 protein family of *Plasmodium* play a role in gamete fertility. *PLoS Pathog.*, 6 (2010), p.
719 e1000853
- 720 6). Van Dijk, M. R. *et al.* A central role for P48/45 in malaria parasite male gamete fertility.
721 (2001) *Cell*, 104(1), pp. 153–164.
- 722 7). van Schaijk, B. C. L. et al. (2006) Pfs47, paralog of the male fertility factor Pfs48/45, is a
723 female specific surface protein in *Plasmodium falciparum*. *Molecular and Biochemical*
724 *Parasitology*, 149(2), pp. 216–222.
- 725
- 726 8). Sinden RE. Developing transmission-blocking strategies for malaria control. *PLoS*
727 *Pathogens* (2017) 13:e1006336.

- 728 9). Sauerwein RW, Bousema T. Transmission blocking malaria vaccines: Assays and
729 candidates in clinical development. *Vaccine*. (2015) Dec 22; 33(52):7476-82.
730
- 731 10). Singh SK, Roeffen W, Andersen G, Bousema T, Christiansen M, Sauerwein, Theisen
732 M.A. *Plasmodium falciparum* 48/45 single epitope R0.6C subunit protein elicits high levels of
733 transmission blocking antibodies. *Vaccine* (2015) Apr 15;33(16):1981-6.
734
- 735 11). Singh SK, Thrane S, Janitzek CM, Nielsen MA, Theander TG, Theisen M, Salanti A,
736 Sander AF. Improving the malaria transmission-blocking activity of a *Plasmodium falciparum*
737 48/45 based vaccine antigen by SpyTag/SpyCatcher mediated virus-like display. *Vaccine*.
738 (2017) Jun 27;35(30):3726-3732.
739
- 740 12). Outchkourov NS, Roeffen W, Kaan A, Jansen J, Luty A, Schuiffel D, van Gemert GJ,
741 van de Vegte-Bolmer M, Sauerwein RW, Stunnenberg HG. Correctly folded Pfs48/45 protein
742 of *Plasmodium falciparum* elicits malaria transmission-blocking immunity in mice. *Proc Natl*
743 *Acad Sci U S A*. 2008 Mar 18;105(11):4301-5.
- 744 13). Outchkourov NS, Roeffen W, Kaan A, Jansen J, Luty A, Schuiffel D, van Gemert GJ,
745 van de Vegte-Bolmer M, Sauerwein RW, Stunnenberg HG. Correctly folded Pfs48/45 protein
746 of *Plasmodium falciparum* elicits malaria transmission-blocking immunity in mice. *Proc Natl*
747 *Acad Sci U S A*. (2008) Mar 18;105(11):4301-5.
748
- 749
- 750 14). Read D, Lensen AH, Begarnie S, Haley S, Raza A, Carter R. Transmission-blocking
751 antibodies against multiple, non-variant target epitopes of the *Plasmodium falciparum*
752 gamete surface antigen Pfs230 are all complement-fixing. *Parasite Immunol*. (1994)
753 Oct;16(10):511-9.
754

- 755 15). Miura K, Takashima E, Deng B, Tullo G, Diouf A, Moretz SE, Nikolaeva D, Diakite M,
756 Fairhurst RM, Fay MP, Long CA, Tsuboi T. Functional comparison of *Plasmodium*
757 *falciparum* transmission-blocking vaccine candidates by the standard membrane-feeding
758 assay. *Infect. Immun.* (2013), 81 pp. 4377-4382
759
- 760 16). Kapulu MC, Da DF, Miura K, Li Y, Blagborough AM, Churcher TS, Nikolaeva D,
761 Williams AR, Goodman AL, Sangare I, Turner AV, Cottingham MG, Nicosia A, Straschil U,
762 Tsuboi T, Gilbert SC, Long CA, Sinden RE, Draper SJ, Hill AV, Cohuet A, Biswas S.
763 Comparative assessment of transmission-blocking vaccine candidates against *Plasmodium*
764 *falciparum*. *Sci Rep.* (2015). 11;5:11193. doi:
765
- 766 17). Bompard A, Da DF, Yerbanga RS, Biswas S, Kapulu M, Bousema T, Lefevre T, Cohuet
767 A, Churcher TS. Evaluation of two lead malaria transmission blocking vaccine candidate
768 antibodies in natural parasite-vector combinations, *Scientific Reports.* (2017), Vol: 7, ISSN:
769 2045-2322
- 770 18). Theisen M, Jore MM, Sauerwein R. Towards clinical development of a Pfs48/45-based
771 transmission blocking malaria vaccine. *Expert Rev Vaccines.* (2017) Apr;16(4):329-336.
772
- 773 100). Farrance, C.E., Rhee, A., Jones, R.M., Musiychuk, K., Shamloul, M., Sharma, S., Mett,
774 V., Chichester, J.A., Streatfield, S.J., Roeffen, W., et al. (2011). A Plant-Produced Pfs230
775 Vaccine Candidate Blocks Transmission of *Plasmodium falciparum*. *Clin Vaccine Immunol*,
776 CVI.05105-05111.
777
- 778 19). Blagborough AM, Sinden RE. *Plasmodium berghei* HAP2 induces strong malaria
779 transmission-blocking immunity *in vivo* and *in vitro*. *Vaccine.* (2009). Aug 20;27(38):5187-94.
780

781 20). Canepa GE, Molina-Cruz A, Yenkoidiok-Douti L, Calvo E, Williams AE, Burkhardt M,
782 Peng F, Narum D, Boulanger MJ, Valenzuela JG, Barillas-Mury C. Antibody targeting of a
783 specific region of Pfs47 blocks *Plasmodium falciparum* malaria transmission. *NPJ Vaccines*.
784 2018 Jul 10;3:26.

785
786 21). Miguel-Blanco, C. et al. Imaging-Based High-Throughput Screening Assay To Identify
787 New Molecules with Transmission-Blocking Potential against *Plasmodium falciparum*
788 Female Gamete Formation. *Antimicrob. Agents Chemother.* (2015).59, 3298–3305

789
790 22). Burrows, J. N. et al. New developments in anti-malarial target candidate and product
791 profiles. *Malar. J.* 16, 26 (2017).

792
793 23). Dicko, A. et al. Efficacy and safety of primaquine and methylene blue for prevention of
794 *Plasmodium falciparum* transmission in Mali: a phase 2, single-blind, randomised controlled
795 trial. *Lancet Infect. Dis.* (2018). Jun;18(6):627-639,

796
797 24). Buchholz, K. et al. Interactions of Methylene Blue with Human Disulfide Reductases and
798 Their Orthologues from *Plasmodium falciparum*. *Antimicrob. Agents Chemother.* (2008) 52,
799 183–191.

800
801 25). Fowler, R. E., Sinden, R. E. & Pudney, M. Inhibitory activity of the anti-malarial
802 atovaquone (566C80) against ookinetes, oocysts, and sporozoites of *Plasmodium berghei*.
803 *J. Parasitol.* (1995) 81, 452–458.

804
805 26). Gwadz, R.W. Malaria: successful immunization against the sexual stages of
806 *Plasmodium gallinaceum*. *Science* (1976). 193, 1150-1151.

807

- 808 27). Carter, R., and Chen, D.H. Malaria transmission blocked by immunisation with gametes
809 of the malaria parasite. *Nature* (1976). 263, 57-60.
810
- 811 28). Goodman AL, Blagborough AM, Biswas S, Wu Y, Hill AV, Sinden RE, Draper SJ. A viral
812 vectored prime-boost immunization regime targeting the malaria Pfs25 antigen induces
813 transmission-blocking activity. *PLoS One*. (2011);6(12):e29428.
814
- 815 29). Jones RM, Chichester JA, Manceva S, Gibbs SK, Musiychuk K, Shamloul M, Norikane
816 J, Streatfield SJ, van de Vegte-Bolmer M, Roeffen W, et al. A novel plant-produced Pfs25
817 fusion subunit vaccine induces long-lasting transmission blocking antibody responses. *Hum*
818 *Vaccin Immunother*. (2015); 11(1):124-32.
819
- 820 30). Sala KA, Angrisano F, Da DF. Taylor IJ. Churcher TS. Blagborough AM. Immunization
821 with Transgenic Rodent Malaria Parasites Expressing Pfs25 Induces Potent Transmission-
822 Blocking Activity. *Scientific Reports*. (2018). Jan 25;8(1):1573.
823
- 824 31). Ali Khan, Mutus B. Protein disulfide isomerase a multifunctional protein with multiple
825 physiological roles. *Front Chem*. (2014) Aug 26;2:70.
826
- 827 32). Noiva R. Protein disulfide isomerase: the multifunctional redox chaperone of the
828 endoplasmic reticulum. *Semin Cell Dev Biol*. (1999) Oct;10(5):481-93.
829
- 830 33). Mahajan B, Noiva R, Yadava A, Zheng H, Majam V, Mohan KV, Moch JK, Haynes JD,
831 Nakhasi H, Kumar S. Protein disulfide isomerase assisted protein folding in malaria
832 parasites. *Int J Parasitol*. (2006) Aug;36(9):1037-48.
833

- 834 34). Mouray E, Moutiez M, Girault S, Sergheraert C, Florent I, Grellier P. Biochemical
835 properties and cellular localization of *Plasmodium falciparum* protein disulfide isomerase.
836 *Biochimie.* (2007) Mar;89(3):337-46.
837
- 838 35). Talman AM, Prieto JH, Marques S, Ubaida-Mohien C, Lawniczak M, Wass MN, Xu T,
839 Frank R, Ecker A, Stanway RS, Krishna S, Sternberg MJ, Christophides GK, Graham DR,
840 Dinglasan RR, Yates JR 3rd, Sinden RE. Proteomic analysis of the *Plasmodium* male
841 gamete reveals the key role for glycolysis in flagellar motility. *Malar J.* (2014) Aug 13;13:315.
842
- 843 36). Wass MN, Stanway R, Blagborough AM, Lal K, Prieto JH, Raine D, Sternberg MJ,
844 Talman AM, Tomley F, Yates J 3rd, Sinden RE. Proteomic analysis of *Plasmodium* in the
845 mosquito: progress and pitfalls. *Parasitology.* (2012) Aug;139(9):1131-45.
846
- 847 37). Bushell E, Gomes AR, Sanderson T, Anar B, Girling G, Herd C, Metcalf T, Modrzynska
848 K, Schwach F, Martin RE, Mather MW, McFadden GI, Parts L, Rutledge GG, Vaidya AB,
849 Wengelnik K, Rayner JC, Billker O. Functional Profiling of a *Plasmodium* Genome Reveals
850 an Abundance of Essential Genes. *Cell.* (2017) Jul 13;170(2):260-272.e8.
851
- 852 38). Schwach F, Bushell E, Gomes AR, Anar B, Girling G, Herd C, Rayner JC, Billker O.
853 PlasmoGEM, a database supporting a community resource for large-scale experimental
854 genetics in malaria parasites. *Nucleic Acids Res.* (2015) Jan;43(Database issue):D1176-82.
855
- 856 39). Gomes AR, Bushell E, Schwach F, Girling G, Anar B, Quail MA, Herd C, Pfander C,
857 Modrzynska K, Rayner JC, Billker O. A genome-scale vector resource enables high-
858 throughput reverse genetic screening in a malaria parasite. *Cell Host Microbe.* (2015) Mar
859 11;17(3):404-413.
860

- 861 40). Tewari R, Dorin D, Moon R, Doerig C, Billker O. An atypical mitogen-activated protein
862 kinase controls cytokinesis and flagellar motility during male gamete formation in a malaria
863 parasite. *Mol Microbiol.* (2005) Dec;58(5):1253-63.
864
- 865 41). Reininger L, Tewari R, Fennell C, Holland Z, Goldring D, Ranford-Cartwright L, Billker
866 O, Doerig C. An essential role for the *Plasmodium* Nek-2 Nima-related protein kinase in the
867 sexual development of malaria parasites. *J Biol Chem.* (2009) Jul 31;284(31):20858-68
868
- 869 42). Dickerhof N, Kleffmann T, Jack R, McCormick S. Bacitracin inhibits the reductive activity
870 of protein disulfide isomerase by disulfide bond formation with free cysteines in the
871 substrate-binding domain. *FEBS J.* (2011) Jun;278(12):2034-43.
872
- 873 43). Fédry, J. *et al.* The Ancient Gamete Fusogen HAP2 Is a Eukaryotic Class II Fusion
874 Protein, *Cell*, (2017) 168, pp. 904–915.
875
- 876 44). Pinello, J. F. *et al.* Structure-Function Studies Link Class II Viral Fusogens with the
877 Ancestral Gamete Fusion Protein HAP2, *Current Biology.* (2017), 27(5), pp. 651–660.
878
- 879 45). Kozlov G, Määttänen P, Thomas DY, Gehring K. A structural overview of the PDI family
880 of proteins. *FEBS J.* (2010) Oct;277(19):3924-36.
881
- 882 46). Benham AM. The protein disulfide isomerase family: key players in health and disease.
883 *Antioxid Redox Signal.* (2012) Apr 15;16(8):781-9.
884
- 885 47). van Lith M, Hartigan N, Hatch J, Benham AM. PDILT, a divergent testis-specific protein
886 disulfide isomerase with a non-classical SXXC motif that engages in disulfide-dependent
887 interactions in the endoplasmic reticulum. *J Biol Chem.* 2005 Jan 14;280(2):1376-83.
888

- 889 48). Turano C, Coppari S, Altieri F, Ferraro A. Proteins of the PDI family: unpredicted non-
890 ER locations and functions. *J Cell Physiol.* (2002) Nov;193(2):154-63.
891
- 892 49). Ellerman DA, Myles DG, Primakoff P. A role for sperm surface protein disulfide
893 isomerase activity in gamete fusion: evidence for the participation of ERp57. *Dev Cell.*
894 (2006) Jun;10(6):831-7.
- 895 50). Primakoff P, Myles DG. Cell-cell membrane fusion during mammalian fertilization. *FEBS*
896 *Lett.* (2007) May 22;581(11):2174-80.
- 897 51). Reiser K, François KO, Schols D, Bergman T, Jörnvall H, Balzarini J, Karlsson A,
898 Lundberg M Thioredoxin-1 and protein disulfide isomerase catalyze the reduction of similar
899 disulfides in HIV gp120. *Int J Biochem Cell Biol.* (2012) Mar;44(3):556-62.
900
- 901 52). Gilbert J, Ou W, Silver J, Benjamin T. Downregulation of protein disulfide isomerase
902 inhibits infection by the mouse polyomavirus. *J Virol.* (2006) Nov;80(21):10868-70.
903
- 904 53). Wan SW, Lin CF, Lu YT, Lei HY, Anderson R, Lin YS. Endothelial cell surface
905 expression of protein disulfide isomerase activates β 1 and β 3 integrins and facilitates
906 dengue virus infection. *J Cell Biochem.* (2012). May;113(5):1681-91.
907
- 908 54). Diwaker D, Mishra KP, Ganju L, Singh SB Protein disulfide isomerase mediates dengue
909 virus entry in association with lipid rafts. *Viral Immunol.* (2015) Apr;28(3):153-60.
910
- 911 55). Taylor M, Burrell H, Banerjee T, Ray S, Curtis D, Tatulian SA, Teter K.
912 Substrate-induced unfolding of protein disulfide isomerase displaces the cholera toxin A1
913 subunit from its holotoxin. *PLoS Pathog.* (2014) Feb; 10(2):e1003925.
914

- 915 56). Santos CX, Stolf BS, Takemoto PV, Amanso AM, Lopes LR, Souza EB, Goto H,
916 Laurindo FR. Protein disulfide isomerase (PDI) associates with NADPH oxidase and is
917 required for phagocytosis of *Leishmania chagasi* promastigotes by macrophages. *J Leukoc*
918 *Biol.* (2009) Oct;86(4):989-98.
919
- 920 57). Wang HL, Li YQ, Yin LT, Meng XL, Guo M, Zhang JH, Liu HL, Liu JJ, Yin GR.
921 *Toxoplasma gondii* protein disulfide isomerase (TgPDI) is a novel vaccine candidate against
922 toxoplasmosis. (*PLoS One*). 2013 Aug 15;8(8):e70884
923
- 924 58). Kushawaha PK, Gupta R, Tripathi CD, Sundar S, Dube A. Evaluation of *Leishmania*
925 *donovani* protein disulfide isomerase as a potential immunogenic protein/vaccine candidate
926 against visceral Leishmaniasis. *PLoS One.* (2012);7(4):e35670.
927
- 928 59). Tsai CW, Duggan PF, Shimp RL Jr, Miller LH, Narum DL. Overproduction of *Pichia*
929 *pastoris* or *Plasmodium falciparum* protein disulfide isomerase affects expression, folding
930 and O-linked glycosylation of a malaria vaccine candidate expressed in *P. pastoris*. *J*
931 *Biotechnol.* (2006) Feb 24;121(4):458-70
932
- 933 60). Ramakrishnan C, Delves MJ, Lal K, Blagborough AM, Butcher G, Baker KW, et al.
934 Laboratory maintenance of rodent malaria parasites. *Methods Mol Biol* (2013);923:51–72.
935
- 936 61). Blagborough AM, Churcher TS, Upton LM, Ghani AC, Gething PW, Sinden RE.
937 Transmission-blocking interventions eliminate malaria from laboratory populations. *Nat*
938 *Commun* (2013);4:1812.
939
- 940 62). Sebastian S, Brochet M, Collins MO, Schwach F, Jones ML, Goulding D, et al. A
941 *Plasmodium* calcium-dependent protein kinase controls zygote development and

942 transmission by translationally activating repressed mRNAs. *Cell Host Microbe* (2012);12(Jul
943 (1)):9–19.

944

945 63). Pfander C, Anar B, Schwach F, Otto TD, Brochet M, Volkmann K, Quail MA, Pain A,
946 Rosen B, Skarnes W, Rayner JC & Billker O. A scalable pipeline for highly effective genetic
947 modification of a malaria parasite. *Nat. Methods* (2011) 8, 1078-1082,

948

949 64). Shookhoff HB. The Present Status of Antibiotics in the Treatment of Protozoan Diseases.
950 *Bull N Y Acad Med.* (1951) Jul; 27(7): 439–451.

951

952 65). Habtewold T, Povelones M, Blagborough AM, Christophides GK. Transmission blocking
953 immunity in the malaria non-vector mosquito *Anopheles quadriannulatus* species A. *PLoS*
954 *Pathog.* 2008 May 23;4(5):e1000070.

955

Figure 1.

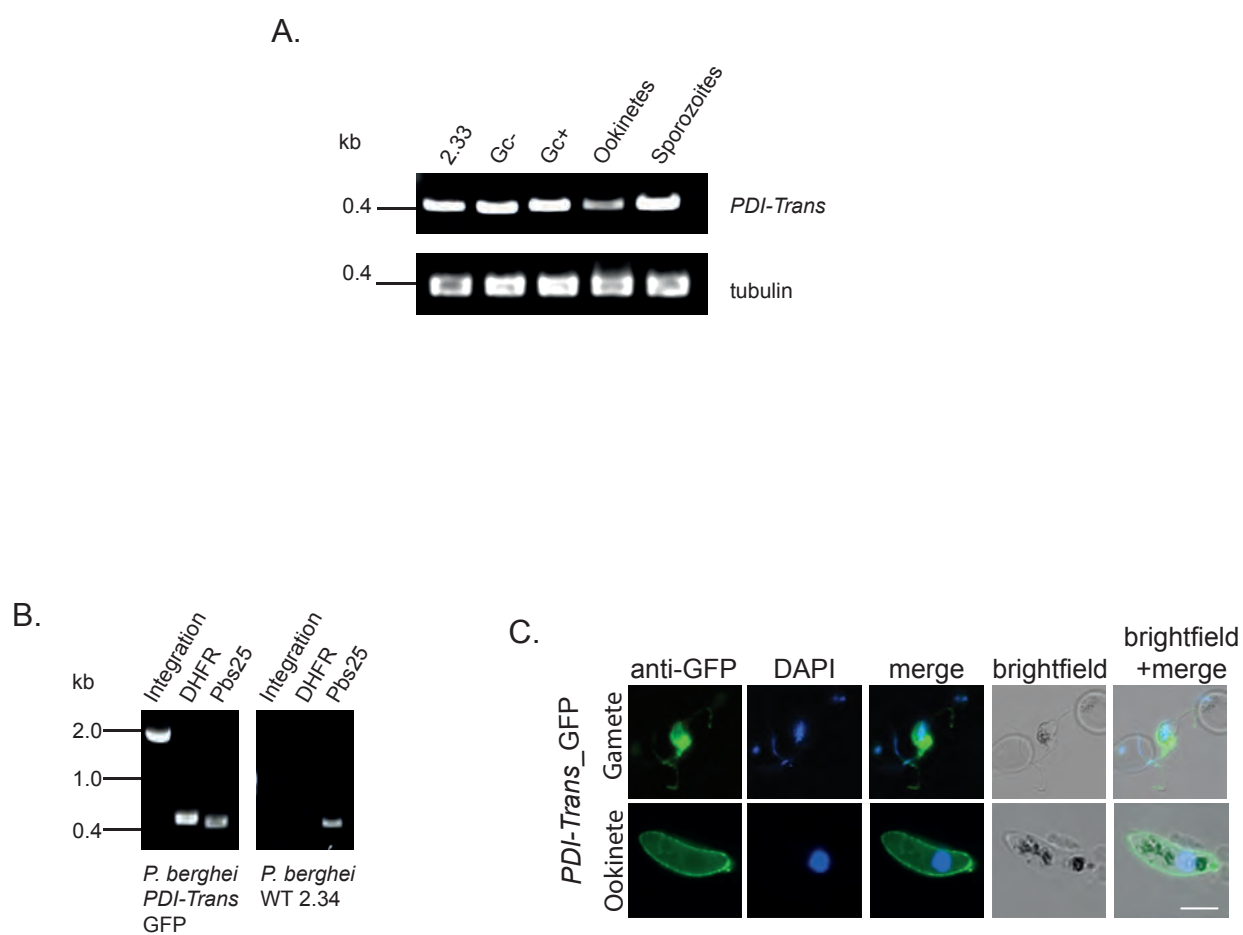


Figure 2.

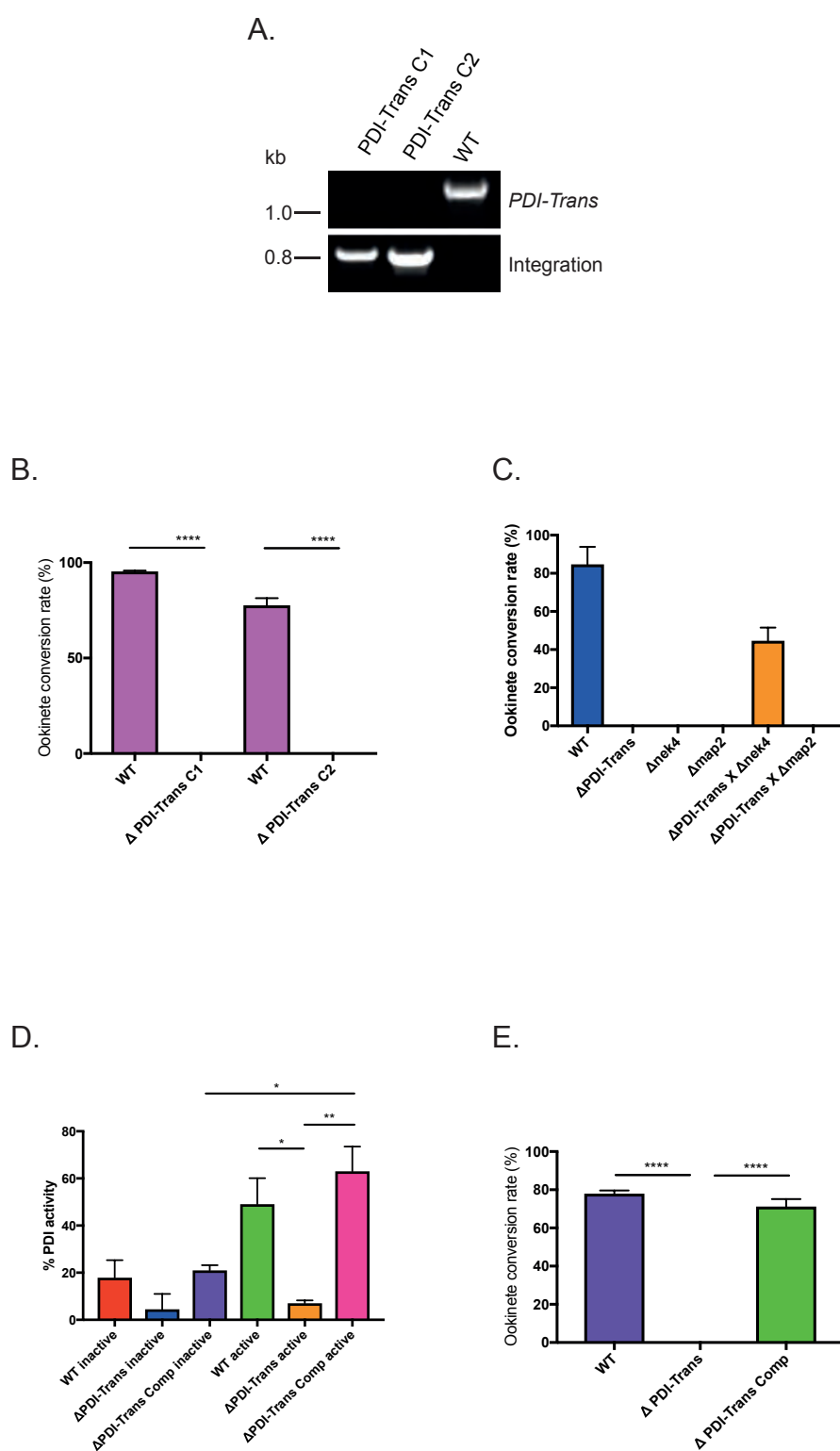


Table 1.

	Wild type	ΔPDI -Trans Clone 1	Wild type	ΔPDI -Trans Clone 2
<i>Mean intensity (n = 3)</i>	59.81	3.19	60.17	2.23
<i>Mean prevalence (n = 3)</i>	92.67	34	93.86	32.67
<i>Inhibition in intensity (%)</i>	-	94.38 ^a	-	96.43 ^a
<i>Inhibition in prevalence (%)</i>	-	63.68 ^b	-	65.62 ^b

Figure 3.

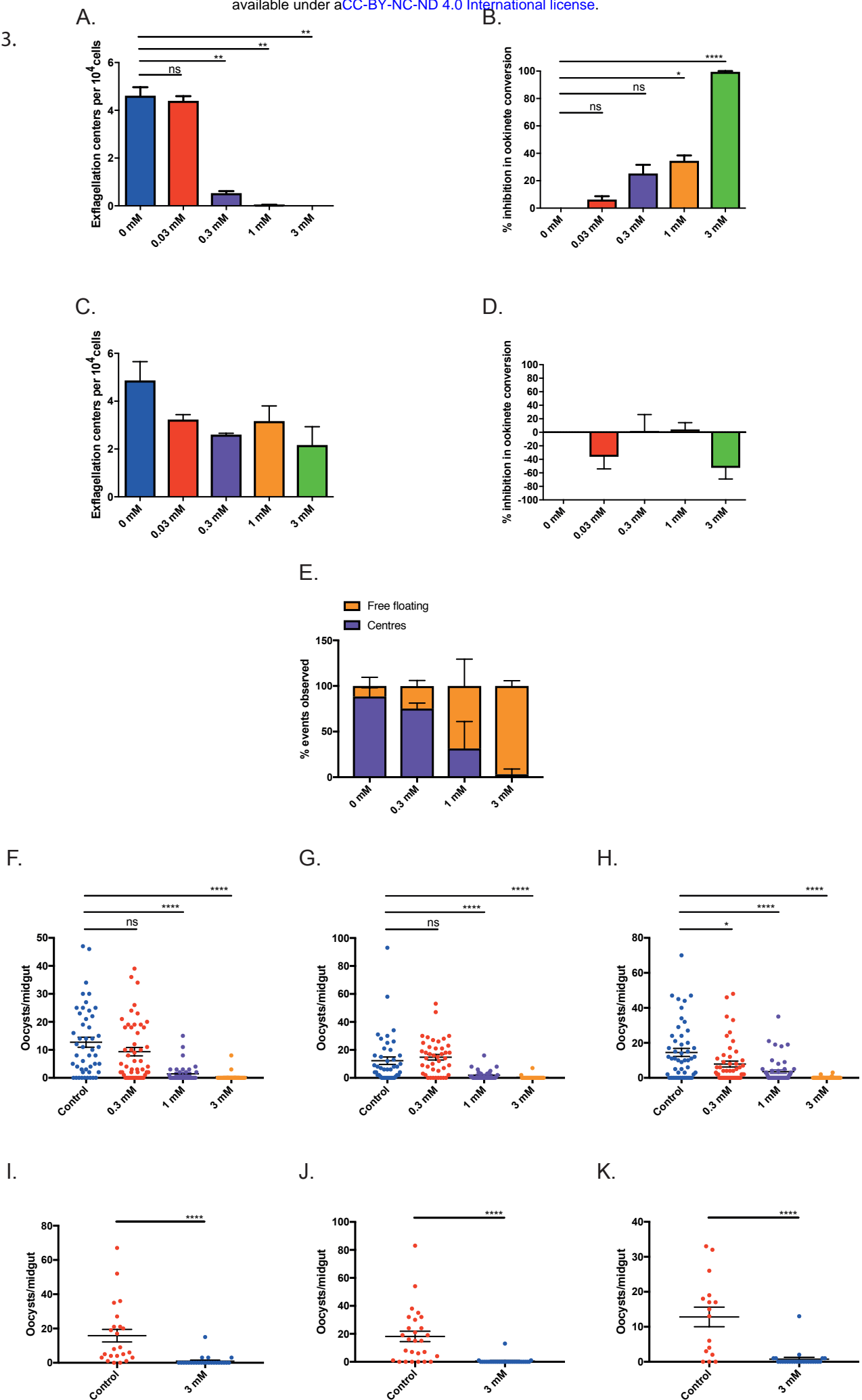


Table 2.

	Control	0.3 mM	1 mM	3 mM
<i>Mean intensity (n = 3)</i>	13.17	10.68	2.32	0.23
<i>Mean prevalence (n = 3)</i>	77.37	72.32	38.29	5.81
<i>Inhibition in intensity (%)</i>	-	17.20 ^a	82.77 ^a	98.21 ^a
<i>Inhibition in prevalence (%)</i>	-	6.72 ^b	50.23 ^b	92.48 ^b

Table 3.

	Control Feed 1	Bacitracin Feed 1	Control Feed 2	Bacitracin Feed 2	Control Feed 3	Bacitracin Feed 3
<i>Mean intensity</i>	15.83	0.96	18.15	0.52	12.81	0.76
<i>Mean prevalence</i>	91.30	16	78.57	10	81.25	20
<i>Inhibition in intensity (%)</i>	-	93.93	-	97.14	-	94.07
<i>Inhibition in prevalence (%)</i>	-	82.48	-	87.27	-	75.38

Figure 4.

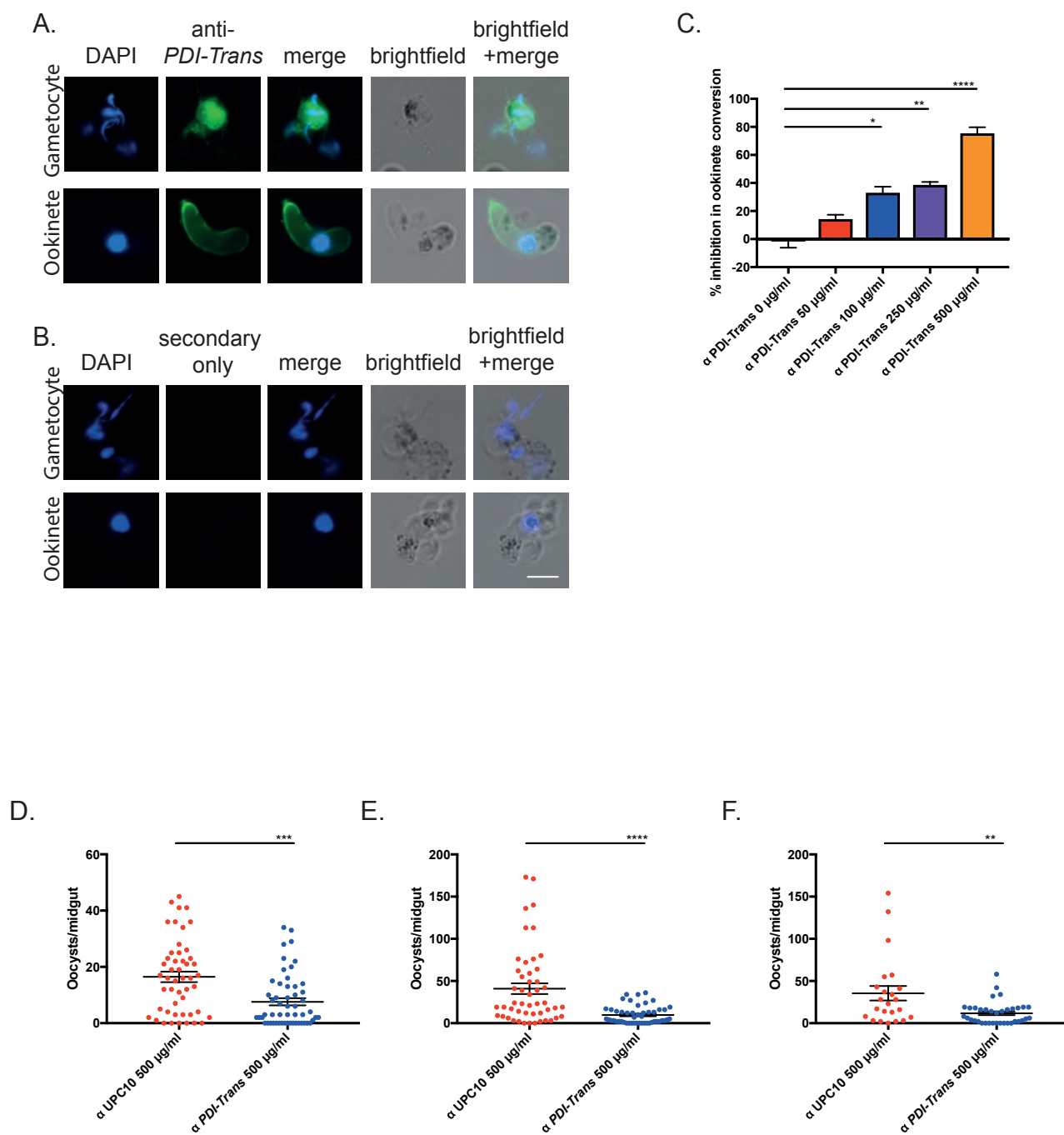
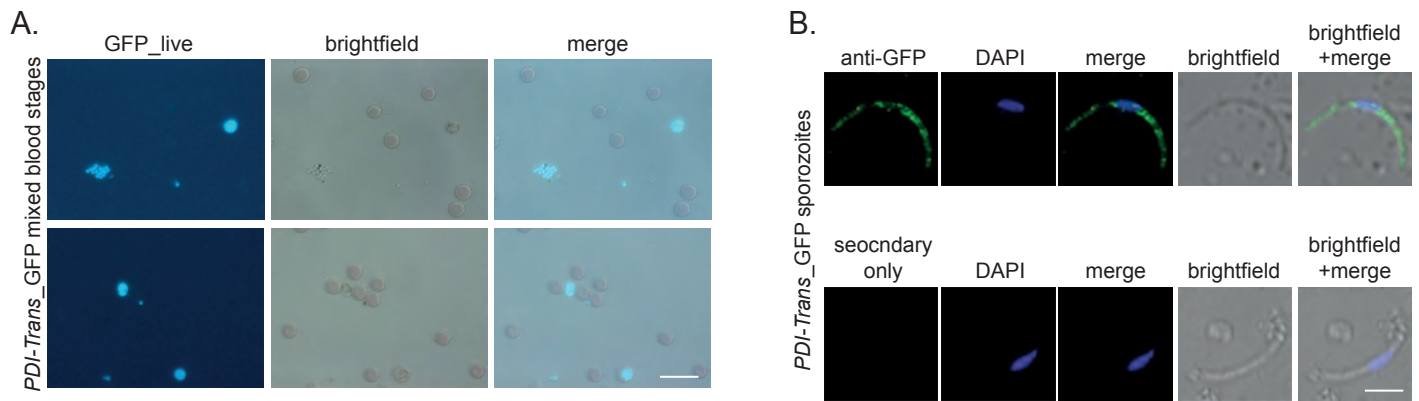


Table 4.

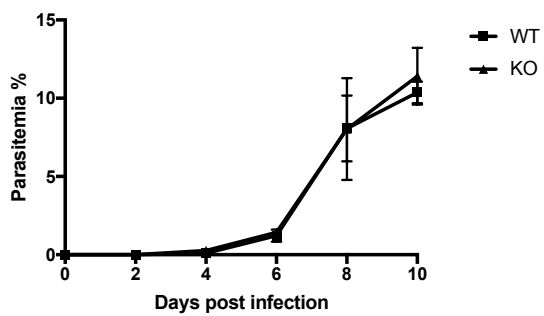
	α UPC10 500 μ g/ml	α PDI-Trans 500 μ g/ml
<i>Mean intensity (n = 3)</i>	31.37	9.82
<i>Mean prevalence (n = 3)</i>	93.28	62.18
<i>Inhibition in intensity (%)</i>	-	66.22 ^a
<i>Inhibition in prevalence (%)</i>	-	33.16 ^b

S1.

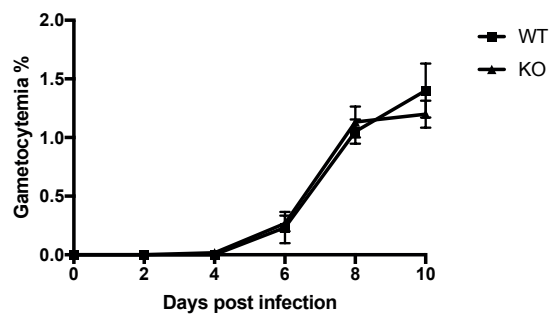


S2.

A.

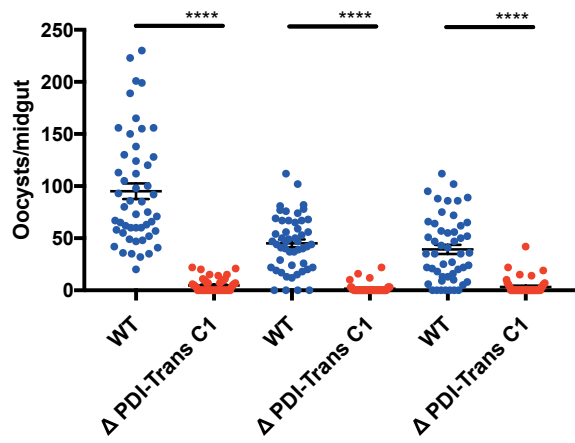


B.

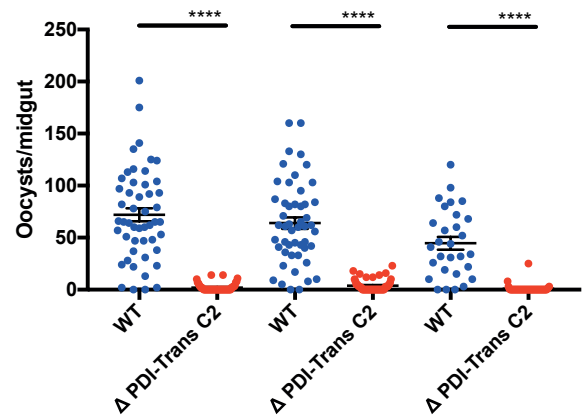


S3.

A.



B.



S4.

